IEEE Access
Multidisciplinary ⋮ Rapid Review ⋮ Open Access Journal

Received 6 November 2023, accepted 16 November 2023, date of publication 20 November 2023,
date of current version 8 December 2023.

*Digital Object Identifier 10.1109/ACCESS.2023.3335242*

RESEARCH ARTICLE

# Multi-Time-Scale Optimal Scheduling of Integrated Energy System Considering Demand Response

**JIAN TANG[1], JIANFENG LIU[1], TIANXING SUN[1], HERAN KANG[1], AND XIAOQING HAO[2]**
[1]Economic and Technological Research Institute, State Grid Inner Mongolia Eastern Electric Power Company Ltd., Hohhot 010020, China
[2]Inner Mongolia Hengsheng New Energy Technology Company Ltd., Baotou 014030, China

Corresponding author: Jianfeng Liu (yph_1025@163.com)

**ABSTRACT** Large-scale new energy access brings certain pressure to the scheduling and operation of the integrated energy system (IES), which will affect the safety and reliability of the system. To address this issue, this paper proposes to deeply excavate the demand response (DR) capability of loads to participate in the scheduling and operation of IES. Firstly, according to the inertia effect of heat load in IES, a multi-time-scale scheduling strategy considering the DR of electric and heat load is proposed, which includes three stages: day-ahead, intra-day upper layer, and intra-day lower layer. Secondly, an optimal scheduling model of IES is established with the aim of minimizing the total operating cost of IES. Among them, the day-ahead stage comprehensively considers the electro-thermal DR to formulate the output plan of the energy supply equipment. The intra-day stage is divided into two time scales: the long-term upper layer and the short-term lower layer to adjust the output of electric and heat energy supply equipment layer by layer to realize the real-time economic operation of IES. Finally, the feasibility of the proposed multi-time-scale scheduling strategy is verified through the case study. The results indicate that the multi-time-scale optimal scheduling, taking into account the DR of electric and heat loads, can improve the accommodation capacity of new energy while ensuring the economic operation of the system.

**INDEX TERMS** Integrated energy system, demand response, multi-time scale, optimal scheduling.

## NOMENCLATURE

*Abbreviations*

| | |
|---|---|
| DR | Demand response. |
| IDR | Integrated demand response. |
| HDR | Heat load demand response. |
| PDR | Price demand response. |
| A-IDR | Transferable demand response. |
| B-IDR | Interruptible demand response. |
| CHP | Combined heat and power. |
| PV | Photovoltaic. |
| WT | Wind turbine. |
| EB | Electric boiler. |
| ES | Energy storage. |
| HS | Heat storage. |
| HSC | Heat storage capability. |
| HSDC | Heat storage discharge capability. |
| ESC | Energy storage capability. |
| ESDC | Energy storage discharge capability. |

*Indices and Sets*

| | |
|---|---|
| $i$ | Index for units. |
| $t$ | Index for time period. |
| $\Omega$ | Set of system energy conversion units type. |
| $\Delta t$ | Scheduling interval. |
| $\mu$ | Unit adjustment costs. |
| $\varphi$ | Output power of device. |
| $C$ | Cost. |
| E | Capacity of the units. |
| P | Electrical power. |
| H | Heat power. |
| Q | Gas power. |

The associate editor coordinating the review of this manuscript and approving it for publication was Diego Bellan.

*Superscripts*

| | |
|---|---|
| *sto* | Storage. |
| *chr* | Charge to ES/HS. |
| *dis* | Discharge from ES/HS. |
| *curt* | Reduction power. |
| *trans* | Transfer power. |
| *on* | Device start. |
| *off* | Device stop. |
| *u* | Operating state of the device. |
| *max* | Maximum value. |
| *min* | Minimum value. |

## I. INTRODUCTION

With the increasing scarcity of fossil fuels and the worsening environmental pollution, the establishment of efficient, clean and multi-energy coupled IES has become crucial to address these problems. IES is based on the utilization of renewable energy sources and integrates various energy sources such as electricity, gas, cooling and heating, aiming to improve energy utilization through the coupling and complementation of multiple energy sources [1]. The coupling and complementarity of the ''source-network-load-storage'' elements in IES enables the system to meet the diverse energy needs of users. At the same time, users can adjust their energy consumption behavior and participate in system scheduling according to their needs. Through interactive and coordinated optimization scheduling between the energy sources and loads, IES can achieve the synergistic, complementary, and economically efficient operation of various heterogeneous energy subsystems [2], [3].

DR is an important way for loads to participate in system dispatching by shifting energy in time through load adjustment to achieve a flattening of the filling curve of the integrated energy system and to adjust up the system operating economy [4]. The traditional DR is only for power users. According to the load demand characteristics of users, it can be divided into transferable load and interruptible load. According to the response form, it can be divided into price demand response (PDR) and incentive demand response (IDR) [5], [6]. Reference [7] introduced PDR into the system cooperative dispatch to stimulate user-side load flexibility and achieve peak-shaving and valley-filling effects. However, with the continuous development of integrated energy sources, the coupling of energy sources with different characteristics deepens, and different types of loads or the same type of loads have different responsiveness under different incentives. Therefore, it is important for IES to fully invoke the flexibility of load-side demand response (DR) and study the participation of different types of DR in scheduling under different energy sources.

With the continuous development of IES ''source-network-load-storage'' collaborative scheduling, DR plays a more and more important role in coordinating energy supply and demand balance and improving energy efficiency [8]. Reference [9] constructed a bilevel programming model based on the PDR model. The upper model takes the maximum profit of the supplier as the objective function, and the lower model takes the minimum emission of IES pollutants as the optimization objective. Based on elastic PDR and consumer benefit function, Reference [10] constructed a model in which consumers change their energy consumption habits with the change of price signal, which provided a theoretical basis for determining the potential of DR. The IES proposed in [11] includes photovoltaic, biomass power generation and DR. The research showed that the transferable load in DR can realize peak cutting and valley filling and reduce operating costs. Reference [12] added PDR to the IES study considering combined heat and power (CHP) to relieve the system power supply pressure by shifting part of the load on the customer side during the electrical peak and to improve the system dispatch flexibility. Reference [13] proposed to consider the DR of heat and cold loads and construct an IES DR model containing electrical, heat, and cold loads. In [14], an IES optimal scheduling model for combined cooling, heating and power supply considering IDR is constructed to effectively reduce the scheduling difficulties caused by system randomness. Reference [15] established an IES economic scheduling model considering DR and validated the optimized scheduling model through numerical simulations. The results showed that considering the DR can reduce the operating cost of the system to a certain extent. Reference [16] established a wind power system optimal scheduling model based on robust programming method, which can formulate different DR plans for different classes of loads, and it is proved that DR can reduce peak load and realize peak cutting and valley filling. The above references proved that the introduction of DR into IES can effectively alleviate the power supply pressure of the system and reduce the operating cost. However, the optimal scheduling of IES with DR is carried out on the same time scale, and the impact of DR on the system under different scheduling time scales is not considered.

The multi-time-scale scheduling problem of IES is increasingly important. Therefore, it is necessary to refine the scheduling time scale step by step to reduce the prediction error, improve the wind and solar accommodation and reduce the system reserve capacity at the same time [17]. At present, there has been extensive research on electro-thermal multi-time-scale collaborative optimal scheduling. Reference [18] divided the interaction process between electric power and heating system into four stages, and each stage was a quasi-steady-state multi-energy flow model, which can reflect the time-scale characteristics of IES. Reference [19] proposed a CCHP micro-grid, which includes a two-stage coordinated dispatching strategy of ''intra-day rolling and real-time feedback'', which has been established to continuously adjust system output to minimize economic costs. Reference [20] proposed a mixed time-scale IES optimal scheduling model based on the interplay of supply and demand games, and it was updated in accordance with the response properties of various energies. The tactic increased the system's economic benefit by striking a balance between economy and resilience. Reference [21] considered the power trading

mechanism and corrected system prediction errors at three time scales: day-ahead, intra-day and real-time, establishing a block chain-based multi-time-scale energy trading system for distribution networks. Reference [22] proposed a multi-spatiotemporal scale optimization operation strategy based on multi-energy supply and demand balance, and constructed a collaborative optimization framework consisting of upper, middle, and lower components. The upper model optimized the whole community in the day-ahead stage, the middle model optimized each community in the intra-day stage, and the lower model optimized the power part of each community in the real-time stage. Reference [23] used electric boilers for thermoelectric decoupling, considered demand-side response, and constructed a multi-time-scale scheduling model for a thermoelectric joint system with the objective function of minimizing system scheduling cost. Reference [24] established a multi-time-scale optimization model considering DR and load power constraints, with the objective function of minimizing user electricity cost and system power fluctuation as the real-time optimization scheduling research strategy. The improved particle swarm optimization algorithm was used to solve the model, which can reduce user electricity costs and system volatility. Reference [25] extended the traditional DR and constructed a day-ahead and intra-day scheduling model considering demand-side response. The above references proved the application of multi-time scale in IES, but there are few references to optimize the scheduling of the system on the basis of considering electro-thermal incentive demand response (IDR). Even if the comprehensive consideration of DR and multi-time-scale is taken into account, there is a lack of guidance or real-time scheduling of day-ahead planning, so that the scheduling results are not global.

The grid connection of new energy and the uncertainty of load bring great challenges to power grid scheduling. Scheduling time has become an important reason affecting the stability of the system. In this paper, based on the consideration of electro-thermal heterogeneous load, an optimal scheduling strategy of electro-thermal IES considering multi-time-scale DR is proposed. This strategy improves the flexibility of electro-thermal coupled cooperative scheduling and improves energy efficiency and economy. The main contributions of this paper are as follows:

1)An optimal scheduling strategy considering multi-time-scale load DR is proposed, and the load side with different characteristics participates in the system's ''peak cutting and valley filling'' scheduling. To a certain extent, the energy is transferred in time and space, which alleviates the energy supply pressure of the system.

2)A three-stage step-by-step optimization strategy of ''day-ahead, intra-day upper layer and intra-day lower layer'' of IES based on DR is established, which improves the consumption level of new energy and realizes the deep participation of DR in optimal scheduling under multi-time scale.

The remainder is organized as follows: Section II proposes a multi-time-scale response strategy for IES considering DR. Section III constructs an IES optimal scheduling model considering different types of DR, including objective functions, constraints and solution algorithms. Sections IV and V respectively present the day-ahead and intra-day optimal scheduling of the IES considering DR. The effectiveness of the proposed strategies is verified through case study. Section VI concludes the paper.

## II. MULTI-TIME-SCALE RESPONSE STRATEGY FOR IES WITH DR

### A. ELECTRO-THERMAL LOAD DR MULTIPLE TIME-SCALE OPTIMAL SCHEDULING

DR refers to the grid through the development of time-of-use tariffs or through incentive compensation to change customer energy use behavior, and then participate in grid interaction to achieve peak and valley reduction, optimize the load curve, and improve system stability. DR was divided into electric and heat DR. Electric DR can be further classified into PDR and IDR, which can respond to grid requirements at different multi-time scales. Heat DR is divided into day-ahead long-term response and intra-day short-term response. Users have a certain response delay when participating in grid scheduling while meeting their own electricity consumption needs and need to be notified in advance. IDR is classified into Class A IDR and Class B IDR according to the duration of advance notification to users. The specific classes are shown in Table 1.

**TABLE 1. Class of electric DR.**

| Class | | Response mechanism | Response time |
|---|---|---|---|
| PDR | | Transfer the energy demand to other periods according to the price signal. | Day-ahead 1h |
| IDR | Class A | According to the drive signal, the energy will be transferred to another period of time. | Day-ahead 1h |
| | Class B | After receiving the interrupt signal, in the interruptible part of the peak of power consumption. | Intra-day 15min |

### B. ELECTRO-THERMAL LOAD DR MODELING

#### 1) PDR

This paper adopts the day-ahead hourly price mechanism to formulate the electricity and gas hourly prices according to the load forecast of the next day. The DR is affected by the price mechanism, and the response of the load can be expressed by the price elasticity coefficient, and then the electric load PDR model is established, as shown below:

$$P^t_{e,PDR} = P^t_{e,0}(1 + E_m \cdot \frac{C^t_m - C^t_{m,0}}{C^t_{m,0}}) \tag{1}$$

where $P^t_{e,PDR}$ represents the post-tariff response electric load demand; $P^t_{e,0}$ represents the pre-response electrical load; $E_m$ represents the elasticity factor; $C^t_{m,0}$ and $C^t_m$ represent the tariff before and after DR, respectively.

#### 2) IDR

In this paper, two types of IDR resources with different response periods are considered. Class A belongs to medium- and long-term resources, which transfer power load through advance planning and participate in system peak regulation. Class B belongs to short-term demand change resources with fast response, generally interruptible load, and participates in scheduling regulation in the process of intra-day real-time scheduling. The DR model of electric load is as follows:

$$\begin{cases} P_e^t = P_{p,e}^t + P_{s,e}^t - P_{c,e}^t \\ P_{s,e}^{\min,t} \le \left|P_{s,e}^t\right| \le P_{s,e}^{\max,t} \\ \sum_{t=1}^{T} P_{s,e}^t = 0 \\ 0 \le P_{c,e}^t \le P_{c,e}^{\max,t} \end{cases} \tag{2}$$

where $P_{p,e}^t$ and $P_e^t$ represent the electric load before and after $t$ times of DR, respectively; $P_{s,e}^t$ represent the electric load transferred at time $t$, transferring into the period is positive, transferring out is negative;$P_{c,e}^t$ represents the amount of load that can be interrupted with compensatory excitation at time $t$;$P_{s,e}^{\min,t}$ and $P_{s,e}^{\max,t}$ represent the minimum and maximum amount of load that can be transferred by the electrical load at time $t$, respectively; $P_{c,e}^{\max,t}$ represents the maximum interruptible load at time $t$ of electric load, which is 10% of the total load.

#### 3) HEAT LOAD DR

In the IES studied in this paper, both electrical and heat loads are involved in the DR, heat energy has a delayed transmission characteristic compared to electrical energy, and the heat load user perception is ambiguous using heat load, and the temperature can fluctuate within a certain range to adjust the heat load [26]. The user's perceived temperature comfort is quantitatively expressed by the Predicted Mean Vote (PMV).

$$\lambda_{PMV} = 2.43 - \frac{3.76(T_s - T_{in}^t)}{M(I_{cl} + 0.1)} \tag{3}$$

where $M$ represents the energy metabolic rate of the human body, and generally 80W/m$^2$; $I_{cl}$ represents heat resistance value of the garment, taken as $0.11(m^2 \cdot ^\circ\mathrm{C})/W$; $T_s$ represents the average temperature of human skin in the comfortable state, taken as 33.5°C; $T_{in}^t$ represents the indoor temperature at time $t$.

By considering PMV for flexible regulation of heat load, the temperature perception during daytime is more sensitive than at nighttime, and the comfort requirement is higher. The range of PMV variation during the day time is as follows:

$$\begin{cases} \left|\lambda_{PMV}\right| \le 0.5, t \in [8:00-19:00] \\ \left|\lambda_{PMV}\right| \le 0.9, t \in [1:00-7:00] \cup [20:00-24:00] \end{cases} \tag{4}$$

The heat load demand is determined by indoor temperature, outdoor temperature and other factors, and the heat balance equation for heat load demand and temperature is [27]:

$$\frac{dT_{in}^t}{dt} = \frac{P_H^t - (T_{in}^t - T_{out}^t)KF}{c_{air}\rho_{air}V} \tag{5}$$

where $T_{out}^t$ represents the outdoor temperature at time $t$; $V$, $F$ and $K$ represent building volume, surface area and heat transfer coefficient, respectively; $c_{air}$ and $\rho_{air}$ represent indoor air specific heat capacity and density, respectively; $P_H^t$ represents the heat load required by users at time $t$.

Due to the heat inertia and the ambiguity of load temperature perception, the heat load DR is also divided into two categories: transferable load and interruptible load. The adjustment of heat load is divided into day-ahead scheduling and intra-day upper-level scheduling response The heat load DR model is shown below:

$$\begin{cases} P_h^t = P_{p,h}^t + P_{s,h}^t - P_{c,h}^t \\ P_{s,h}^{\min,t} \le \left|P_{s,h}^t\right| \le P_{s,h}^{\max,t} \\ \sum_{t=1}^{T} P_{s,h}^t = 0 \\ 0 \le P_{c,h}^t \le P_{c,h}^{\max,t} \end{cases} \tag{6}$$

where $P_{p,h}^t$ and $P_h^t$ represent the heat load at time $t$ before and after the DR, respectively; $P_{s,h}^t$ represents the heat load transferred at time $t$ which is positive when transferred to this period and negative when transferred out; $P_{c,h}^t$ represents the heat load reduced at time $t$; $P_{s,h}^{\min,t}$ and $P_{s,h}^{\max,t}$ represent the minimum and maximum transferable load quantities of the heat load at time $t$, respectively, representing 15% of the total load;, $P_{c,h}^{\max,t}$ represents the maximum interruptible load of the heat load at time $t$ and 10% of the total load.

### C. MULTI-TIME-SCALE OPTIMAL SCHEDULING

The user load is uncertain with the change of external environmental factors, and the output of renewable energy also has strong volatility, which puts forward higher requirements for the scheduling plan and security and stability of the system. Therefore, short time scale adjustment of unit output is required to accurately and quickly stabilize the fluctuation of load users and renewable energy output.

With the continuous improvement of new energy and load forecasting accuracy, the smaller the time scale, the smaller the forecasting error and the smaller the uncertainty disturbance to the system. Load resources are scheduled in multi-time scales, and different time scales are scheduling through multi-time-scale coordination and refinement strategies, so as to achieve safe and stable operation of the system and improve the new energy acceptance capacity of the system.

The multi-time-scale scheduling strategy proposed in this paper includes a day-ahead long-time-scale scheduling plan, intra-day upper-layer scheduling and lower-layer real-time adjustment. The multi-time optimal scheduling relationship flow is shown in Fig. 1.

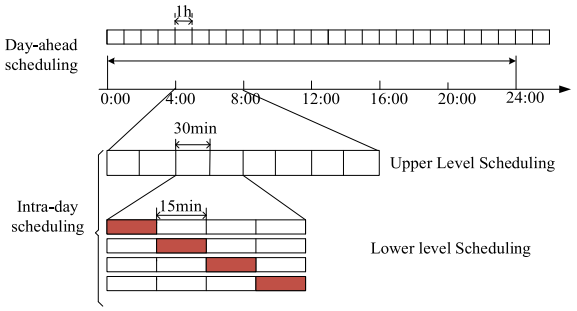


**FIGURE 1.** Day-ahead and Intra-day scheduling time scale strategy chart.

#### 1) DAY-AHEAD OPTIMAL SCHEDULING

Based on the day-ahead forecast of renewable energy and load demand and the electricity price data, taking the lowest operation and maintenance cost of the system as the objective function, and considering the constraints of each equipment, the start-up and shutdown plan and output of each unit for 24 periods a day with 1 hour as the scheduling time scale, as well as the operation plan of energy storage equipment.

#### 2) INTRA-DAY OPTIMAL SCHEDULING

On the basis of day-ahead scheduling, intra-day optimization enables more accurate tracking of renewable energy output and customer load fluctuations by shortening the dispatching cycle. The intra-day optimal scheduling is divided into long and short time scales to guide the hierarchical response of different classes of loads.

The intra-day upper-layer dispatching uses 30mins as the time resolution to predict and update the daily load and the output of renewable energy, and calculates and controls the operation status of each equipment in the next 4 hours according to the day-ahead optimal adjustment value. A rolling optimization plan is executed every 30 minutes to continuously adjust the equipment output to the predicted value. Complete the modification of the day-ahead scheduling plan by rolling backward optimization.

The real-time optimization of the lower layer of the day is based on the rolling optimization results of the upper layer, and the prediction data resolution and scheduling time are adjusted every 15 minutes. Real-time optimization is carried out with the goal of minimizing the sum of power adjustment rates of equipment in all time periods, further reducing prediction errors, improving tracking of load fluctuations, and achieving smooth and economic operation of equipment Considering the construction of DR optimized scheduling model.

## III. CONSIDERING THE CONSTRUCTION OF DR OPTIMIZED SCHEDULING MODEL

### A. BASIC STRUCTURE OF ELECTRO-THERMAL IES

In this paper, an electro-thermal IES model is constructed, as shown in Fig. 2. The electric-thermal integrated energy system studied in this paper consists of two parts, mainly including the power supply part and the heat supply part. The generator sets include photovoltaic (PV), wind power (WP) and combined heat and power (CHP). The main heating equipment includes an electric boiler (EB) and a CHP unit. Energy storage equipment includes energy storage (ES) and heat storage (HS). The electro-thermal IES can flexibly exchange energy with external electricity and gas energy markets.

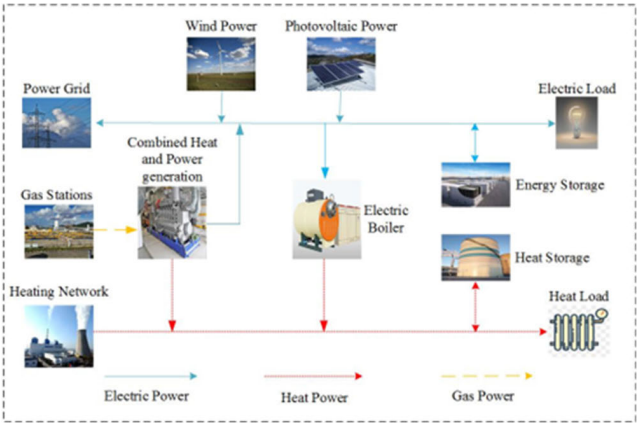


**FIGURE 2.** Structure diagram of power and heat IES.

In the electro-thermal IES, the power subsystem and heat subsystem are coupled between the systems through the CHP unit and the electric-to-heat unit. The CHP unit provides electric energy and heat energy to the power system and heat system respectively, and the electric-to-heat equipment consumes electric energy and produces heat energy at the same time, which realizes the two-way transmission of energy. By adjusting the output of different classes of units at the heat source nodes and adding heat storage devices, the coupling between electricity and heat can be realized.

#### 1) WP GENERATION

The physical model of WP generator is as follows:

$$P_{WT}^{t} = \begin{cases} 0 & v < v_{in} \text{or} v > v_{out} \\ \dfrac{P_{WT,N}(v - v_{in})}{v_N - v_{in}} & v_{in} \le v(\text{t}) \le v_N \\ P_{WT,N} & v_N \le v(\text{t}) \le v_{out} \end{cases} \tag{7}$$

where $P_{WT}^{t}$ represents the output power of the wind turbine; $P_{WT,N}$ represents the rated output power of the fan; $v$, $v_{in}$, $v_N$ and $v_{out}$ represent the actual wind speed, the cut in wind speed, the rated wind speed and the cut out wind speed of the fan, respectively.

#### 2) PV POWER GENERATION

Temperature and light intensity both affect PV's ability to generate power. Here is the mathematical model:

$$P_{PV}^{t} = \alpha_{PV} P_{PV,N} \frac{A_t}{A_S} \left[1 + \alpha_T (T - T_{stp})\right] \tag{8}$$

where $\alpha_{PV}$ represents the derating coefficient; $P_{PV,N}$ represents the rated power of PV (kW); $A_t$ represents the actual

irradiation amplitude of PV at the time $t$, (kW/m$^2$); $A_S$ represents the standard irradiation amplitude, (kW/m$^2$); $\alpha_T$ represents the temperature coefficient; $T_{stp}$ represents the temperature under standard conditions.

#### 3) CHP UNIT

CHP generates both electricity and heat by consuming gas, and its simplified physical model is as follows:

$$\begin{cases} P^t_{CHP} = G^t_{CHP} \cdot \eta_{CHP} \\ H^t_{CHP} = P^t_{CHP} \cdot k_{CHP} \end{cases} \tag{9}$$

where $P^t_{CHP}$ and represent the electrical power and heat power output by the gas turbine; $G^t_{CHP}$ represents input gas volume for the gas turbine; $\eta_{CHP}$ represents the power generation efficiency of the gas turbine; $k_{CHP}$ represents the thermoelectric ratio.

#### 4) EB

The physical model of the EB is as follows:

$$H^t_{EB} = \eta_{EB} P^t_{EB} \tag{10}$$

where $H^t_{EB}$ represents the heat output power of the EB in t period, kW; $P^t_{EB}$ represents the electric power consumed of the EB in $t$ period, kW; $\eta_{EB}$ represents the energy conversion efficiency of the EB.

#### 5) ES

The physical models of ES and heat storage tank have something in common, as shown in the following formula:

$$E^t_{sto} = E^{t-1}_{sto} + (\eta_{sto.chr} P^t_{sto.chr} - P^t_{sto.dis}/\eta_{sto.dis})\Delta t \tag{11}$$

where $E^t_{sto}$ and $E^{t-1}_{sto}$ represent the capacity of the ES at the time of $t$ and $t$-1, respectively; $P^t_{sto.chr}$ and $P^t_{sto.dis}$ represent the charging and discharging power of the ES, respectively; $\eta_{sto.chr}$ and $\eta_{sto.dis}$ represent the charging and discharging efficiency of the ES, respectively; $\Delta t$ represents the scheduling interval.

### B. DAY-AHEAD OPTIMAL OPERATION MODEL

Based on DR's multi-time-scale response strategy, the multi-time-scale optimal operation model of electro-thermal IES is established. The scheduling time is divided into day-ahead, intra-day upper layer and intra-day lower layer. Through the reasonable arrangement of the unit output by the day-ahead optimal scheduling, in order to ensure the economic operation of the system, the objective function is optimized with the lowest total operating cost of the system, the scheduling time is 1 hour and the scheduling cycle is 1 day.

#### 1) OBJECTIVE FUNCTION

$$C = \min\left\{C_{\text{buy}} + C_Q + C_{yun} + C_{DR}\right\} \tag{12}$$

where $C_{\text{buy}}$ represents the cost of purchasing energy from the system, including electricity purchase and gas purchase; $C_Q$ represents the penalty cost of discarding wind and PV power, $C_{yun}$ represents the equipment scheduling operation and maintenance cost, and $C_{DR}$ represents the call cost after considering the load DR adjustment.

Energy purchase cost is as follows:

$$C_{buy} = C_{power} + C_{gas} = \sum_{t=1}^{T} (r^t_e P^t_{e,\text{buy}} + r^t_g Q^t_{g,\text{buy}}) \tag{13}$$

where $C_{power}$ and $C_{gas}$ represent the cost of purchasing electricity and gas, respectively; T represents the scheduling time scale, which is 24h; $r^t_e$ and $r^t_g$ represent the electricity price and gas price, respectively; $P^t_{e,\text{buy}}$ and $Q^t_{g,\text{buy}}$ represent the electric energy and gas energy purchased from the external market during the T period of the system.

Punishment cost of abandoning wind and PV power are as follows:

$$C_Q = \sum_{t=1}^{T} C^{pen}(P^t_{WP,curt} + P^t_{\text{PV},curt}) \tag{14}$$

where $C^{pen}$ represents the penalty coefficient for renewable energy reduction; $P^t_{WP,curt}$ and $P^t_{\text{PV},curt}$ represent WP and PV power generation reduction power, respectively.

Equipment operation and maintenance costs are as follows:

$$\begin{cases} C_{yun} = \sum_{t=1}^{T} (\sum_{i=\Omega} C^i_{on} u^t_i (1 - u^{t-1}_i) + \sum_{i=\Omega} C^i_{off} u^{t-1}_i (1 - u^t_i) \\ + \sum_{i=\Omega} C^i_w P^t_i) \\ \Omega = \{CHP, EB, ES, HS\} \end{cases} \tag{15}$$

where $C^i_{on}$, $C^i_{off}$ and $C^i_w$ represent the start-stop and maintenance cost coefficient of the $i$ device respectively; $u^t_i$ represents the operating state of the $i$ device in binary at time $t$; $P^t_i$ represents the power of the $i$ device in $t$ period.

Call cost after considering load DR is as follows:

$$C_{IDR} = \sum_{t=1}^{24} (C^t_{IDR+} \cdot P^t_{e,IDR+} + C^t_{IDR-} \cdot P^t_{e,IDR-}) \tag{16}$$

where $C_{IDR}$ represents the response cost of IDR; $P^t_{e,IDR+}$ and $C^t_{IDR+}$ represent the increased power load of DR and the corresponding price compensation at time $t$, respectively; $P^t_{e,IDR-}$ and $C^t_{IDR-}$ represent the reduced electrical load and corresponding price compensation at time $t$, respectively.

#### 2) CONSTRAINT CONDITION

Constraints of power balance are as follows:

$$P^t_{WT} + P^t_{PV} + P^t_{CHP} + P^t_{bt.dis} + P^t_{buy} = P^t_{load} + P^t_{EB} + P^t_{bt,chr} \tag{17}$$

$$H^t_{CHP} + H^t_{EB} + H^t_{tst.dis} = H^t_{load} + H^t_{tst.chr} \tag{18}$$

where $P^t_{bt,chr}$ and $P^t_{bt.dis}$ represent the charging and discharging power of the battery (kW); $P^t_{buy}$ represents purchase power from the system (kW); $P^t_{load}$ represents the load power

(kW). $H^t_{tst.chr}$ and $H^t_{tst.dis}$ represent the heat storage tank charging and exothermic power, respectively (kW); $H^t_{load}$ represents the heat load (kW).

Output constraints of equipment are as follows:

$$\varphi_i^{\min} \le \varphi_i^t \le \varphi_i^{\max} \tag{19}$$

where the device $i$ includes CHP unit and EB; $\varphi_i^{\max}$ and $\varphi_i^{\min}$ represent the upper and lower limits of the output power of the device $i$, respectively.

Climbing constraints of equipment are as follows:

$$\varphi_i^{down} \le \varphi_i^t - \varphi_i^{t-1} \le \varphi_i^{up} \tag{20}$$

where $\varphi_i^t$ and $\varphi_i^{t-1}$ represent the output power of device $i$ at the time of $t$ and $t$-1, respectively; and represent the uphill and downhill climbing rates of the equipment i.

Constraints of electro-thermal IES on energy purchase from power grid and gas network are as follows:

$$\begin{cases} P_{\text{buy,min}} \le P^t_{e,\text{buy}} \le P_{buy,\max} \\ Q_{\text{buy,min}} \le Q^t_{g,\text{buy}} \le Q_{buy,\max} \\ P_{\text{buy,dowm}} \le P^t_{e,\text{buy}} - P^{t-1}_{e,\text{buy}} \le P_{buy,\text{up}} \\ Q_{\text{buy,dowm}} \le Q^t_{g,\text{buy}} - Q^{t-1}_{g,\text{buy}} \le Q_{buy,\text{up}} \end{cases} \tag{21}$$

where $P^t_{e,\text{buy}}$ and $Q^t_{g,\text{buy}}$ represent the amount of electricity and gas purchased by the system from the power grid, respectively (kW); $P_{buy,\min}$ and $P_{buy,\max}$ represent the maximum and minimum values of the system power purchase, respectively (kW); $Q_{buy,\min}$ and $Q_{buy,\max}$ represent the maximum and minimum values of the system gas purchase, respectively (kW); $P_{buy,\text{dowm}}$ and $P_{buy,\text{up}}$ represent the climbing value when the system purchases power from the grid, respectively (kW); $Q_{buy,\text{dowm}}$ and $Q_{buy,\text{up}}$ represent the climbing value of the system when purchasing gas from the grid, respectively (kW).

Balance constraints of renewable energy are as follows:

$$\begin{cases} P^t_{\text{WP,av}} = P^t_{WP} + P^t_{WP,curt} \\ P^t_{\text{PV,av}} = P^t_{PV} + P^t_{PV,curt} \end{cases} \tag{22}$$

where $P^t_{\text{WP,av}}$ and $P^t_{\text{PV,av}}$ represent the predicted power of WP and PV units, respectively (kW); $P^t_{WP}$ and $P^t_{PV}$ represent the actual output of WP and PV units in t period, respectively(kW); $P^t_{WP,curt}$ and $P^t_{\text{PV},curt}$ represent the reduction power of WP and PV units in the time period, respectively (kW).

Operation constraints of ES are as follows:

The battery can realize the conversion of electric energy and chemical energy according to the system requirements. The constraints are as follows:

$$\begin{cases} E_{sto}^{\min} \le E_{sto}^t \le E_{sto}^{\max} \\ u^t_{sto} P_{sto}^{\min} \le P^t_{sto,chr} \le u^t_{sto} P_{sto}^{\max} \\ (1-u^t_{sto}) P_{sto}^{\min} \le P^t_{sto,dis} \le (1-u^t_{sto}) P_{sto}^{\max} \\ E^0_{sto} = E^{24}_{sto} \end{cases} \tag{23}$$

where $E_{sto}^{\max}$ and $E_{sto}^{\min}$ represent the upper and lower limits of ES capacity, respectively; $P_{sto}^{\max}$ and $P_{sto}^{\min}$ represent the upper and lower limits of the charging and discharging power of the ES, respectively; $u^t_{sto}$ represents the 0-1 variable; $u^t_{sto} = 1$ represents the charging state; $u^t_{sto} = 0$ represents the state of release; $E^0_{sto}$ and $E^{24}_{sto}$ represent the capacity of the ES at the beginning and end of the scheduling cycle, respectively, to ensure that the content of the ES in a scheduling cycle remains unchanged.

Constraints of DR are as follows:

$$\begin{cases} 0 \le P^t_{e,PDR} \le P^{\max}_{e,PDR} \\ 0 \le P^t_{e,AIDR+} \le P^{\max}_{e,AIDR+} \\ 0 \le P^t_{e,AIDR-} \le P^{\max}_{e,AIDR-} \end{cases} \tag{24}$$

where $P^t_{e,PDR}$ represents the response load under the time-of-use electricity price; $P^{\max}_{e,PDR}$ represents the maximum value of PDR response; $P^{\max}_{e,AIDR+}$ and $P^{\max}_{e,AIDR-}$ represent the maximum value of the increase and decrease of Class A IDR.

### C. INTRA-DAY OPTIMAL SCHEDULING

Due to the difference in response speed of different energy sources and devices, there is a problem of whether the response time level matches the running time scale. Therefore, based on the DR multi-time-scale response strategy, on the basis of day-ahead scheduling, the system is divided into long and sectional time scales in the day-ahead scheduling, the upper layer optimizes the heat DR on a long time scale, adjusts the equipment with long response time such as CHP and heat storage, and the lower layer optimizes the electricity demand and adjusts the related equipment with fast response such as electric boilers and batteries.

#### 1) INTRA-DAY LONG-TIME SCHEDULING CYCLE

The intra-day upper-layer scheduling takes 30 minutes as the time scale, considers the role of heat load DR on the demand side, and the intra-day adjustment cost of setting the target function as IES is the lowest.

Objective function:

The objective function of the intra-day long time scale period in the upper layer is shown as follows:

$$C_{upper} = \min \sum_{t=1}^{24} C_{h,upper} \tag{25}$$

where $C_{upper}$ represents the upper-layer scheduling cost; $C_{h,upper}$ represents the scheduling cost of heating equipment, including CHP unit, EB and HS equipment.

$$C_{h,upper} = \left[\mu_{CHP}(\Delta H^t_{CHP})^2 + \mu_{EB}(\Delta H^t_{EB})^2 + \mu_{HS}(\Delta H^t_{HS})^2\right] \Delta t_1 \tag{26}$$

where $\Delta H^t_{CHP}$, $\Delta H^t_{EB}$ and $\Delta H^t_{HS}$ represent the output power adjustment values of the heating equipment in t period, respectively; $\mu_{CHP}$, $\mu_{EB}$ and $\mu_{HS}$ represent the unit adjustment costs of heating equipment; $\Delta t_1$ represents the upper-layer scheduling time, which is 0.5h.

Constraint condition:

In the upper-layer optimization cycle, the heat equipment constraints are the same as the day-ahead, and the intra-day upper heat energy DR constraints are as follows:

$$\Delta P_{DR,h}^{\min} \le \Delta P_{DR,h}^{t} \le \Delta P_{DR,h}^{\max} \tag{27}$$

where $\Delta P_{DR,h}^{\min}$ and $\Delta P_{DR,h}^{\max}$ represent the upper and lower limits of the heat DR response.

#### 2) SHORT SCHEDULING CYCLE OF LOWER LAYER

Based on the day-ahead plan and intra-day upper-level adjustment, considering the rapid response of electric energy, the intra-day lower layer takes 15min as the time scale, sets the objective function as IES to minimize the adjustment cost, and considers the role of class B IDR on the demand side.

Objective function:

The objective function of the lower power adjustment period is as follows:

$$C_{lower} = \min \sum_{t=1}^{24} (C_{e,lower} + C_{BIDR}) \tag{28}$$

where $C_{lower}$ represents the adjustment cost of periodic electro-thermal IES in the intra-day lower layer; $C_{e,lower}$ represents the power supply equipment adjustment cost; $C_{BIDR}$ represents the class B IDR response cost.

$$\begin{aligned} C_{e,lower} = [&C_{e,grid}^{t} \cdot \Delta P_{grid}^{t} + \mu_{grid}(\Delta P_{grid}^{t})^2 \\ &+ \mu_{CHP}(\Delta P_{CHP}^{t})^2 + \mu_{ES}(\Delta P_{ES}^{t})^2]\Delta t_2 \end{aligned} \tag{29}$$

where $\Delta P_{grid}^{t}$ represents the adjustment value of electricity purchased from the power grid by IES in the $t$ period; $\Delta P_{CHP}^{t}$ and $\Delta P_{ES}^{t}$ represent the output power adjustment value of power supply equipment in the $t$ period, respectively; $\mu_{grid}$, $\mu_{CHP}$ and $\mu_{ES}$ represent unit adjustment costs of the supply unit and equipment, respectively; $\Delta t_2$ represents the time scale of the lower cycle, which is 15 minutes.

$$C_{BIDR} = \sum_{t=1}^{24} (C_{CAP} \cdot P_{e,BIDR}^{\max} + C_{BIDR}^{t} \cdot P_{e,BIDR}^{t}) \tag{30}$$

where $C_{CAP}$ represents the capacity price; $P_{e,BIDR}^{\max}$ represents the interruptible load; $C_{BIDR}^{t}$ represents the price of energ; $P_{e,BIDR}^{t}$ represents the actual power outage.

Constraint condition:

In the lower optimization cycle, the power balance constraints, equipment constraints and tie line constraints are consistent with the day ahead. The interruptible load constraints are adjusted as follows:

$$0 \le P_{e,BIDR}^{t} \le P_{e,BIDR}^{\max} \tag{31}$$

where $P_{e,BIDR}^{\max}$ represents the maximum interruptible load of class B IDR.

**TABLE 2. Operation data of system units.**

| Parameter class | CHP | EB | ES | HS |
|---|---|---|---|---|
| Upper limit of power | 200 | 200 | 500 | 500 |
| Lower limit of power | 20 | 0 | 30 | 20 |
| Climbing rate | 50 | 250 | 400 | 400 |
| Efficiency | 0.85 | 0.95 | 0.99 | 0.95 |

### D. SOLVING PROCESS OF MULTI-TIME-SCALE OPTIMAL OPERATION OF ELECTRO-THERMAL IES

In this paper, a multi-time-scale scheduling model of electro-thermal IES taking into account DR is constructed. The optimal operation model is divided into three scheduling stages: day-ahead-intra-day upper-day-ahead lower layer. Through multi-time-scale cooperation step by step, the system scheduling accuracy and operation stability are improved. The solution of the model belongs to the mixed integer linear optimal programming problem. By establishing the model in MATLAB, the CPLEX solver in the YALMIP toolbox is used to optimize the model, searching for the optimal DR and unit output, so that the economic cost of the model is the lowest and the scheduling flexibility is better. The specific optimization scheduling process is shown in Fig. 3:

## IV. ANALYSIS OF DAY-AHEAD OPTIMAL SCHEDULING

### A. SYSTEM PARAMETERS AND SCENE SETTINGS

The IES of a small park is selected as the research object. The system takes new energy as the main energy supply. The typical winter electricity, heat load, wind power, and photovoltaic predictions for the region are shown in Fig. 4, and the relevant parameters of the system unit are shown in Table 2. Consider introducing the multi-time-scale DR into the park IES, and study its impact on the optimal scheduling of electro-thermal IES, which is verified by scenario analysis.

### B. SYSTEM PARAMETERS AND SCENE SETTINGS

#### 1) 4.2.1 DR ANALYSIS

During the day-ahead optimization operation process, the electric energy DR will be considered to adjust the electric load of PDR and Class A IDR. Heat DR is divided into transferable heat load and interruptible heat load. Fig. 5 and Fig. 6 show the day-ahead load DR after considering electric DR and heat DR, respectively.

According to the analysis, under the action of time-of-use electricity price, the change of electricity load is consistent with the change of price: at the peak of load, the price is raised, and the load is transferred to other times to achieve peak cutting. When the load is low, the price decreases appropriately, and the peak load is transferred to this period, and the valley filling is realized. This shows that considering PDR can affect the load by adjusting the price. Under the price incentive compensation mechanism, the load is interrupted

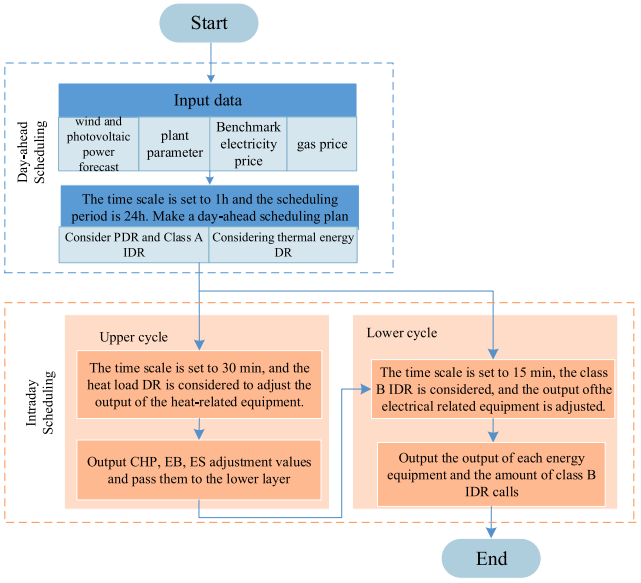


**FIGURE 3.** System optimization scheduling flow chart.

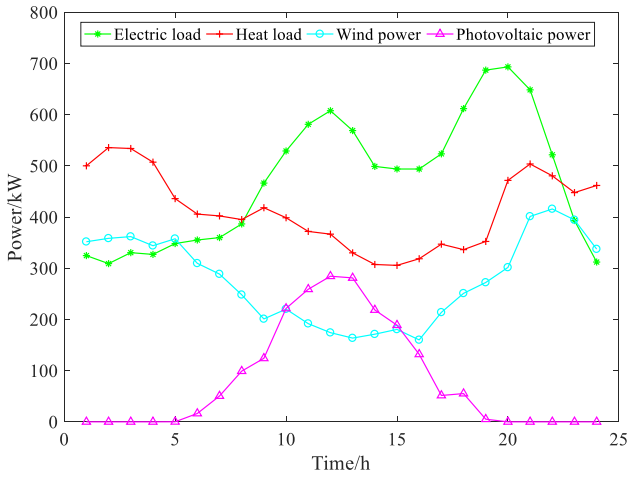


**FIGURE 4.** Predicted output value.

in advance. When the load is at the peak of energy supply, the compensation price is higher and the load interruption is more. When the load is low, the compensation price is low and the load response is less. Under the joint action of time-of-use electricity price and incentive compensation, the load peak-valley difference has been smoothed out and the pressure on the system during peak energy consumption has been alleviated.

Heat DR is realized by users' fuzzy perception of temperature and time-delay inertia of heat energy. As can be seen from Fig. 6, the overall situation is equivalent to the transfer of the heat load on a time scale to some extent. When the power load is at its peak, the heat load demand decreases, which can alleviate the system operation pressure. During the day, the light energy is surplus and the temperature is high, and the heat load demand is low, so the heat is stored in advance. Heat is released during the peak period of heat load at night. In this way, the appropriate transfer and interruption of the

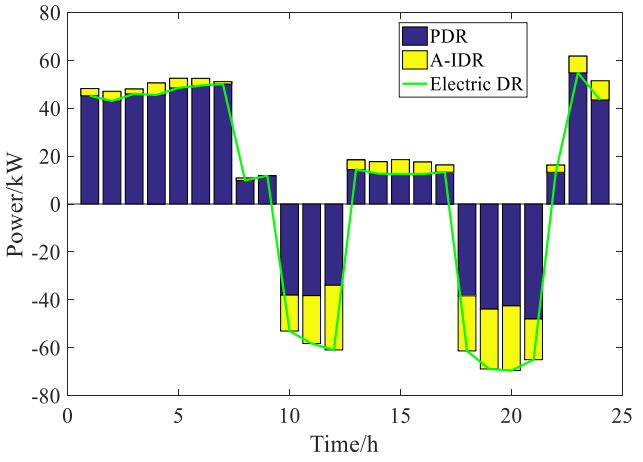


**FIGURE 5.** Electricity load DR.

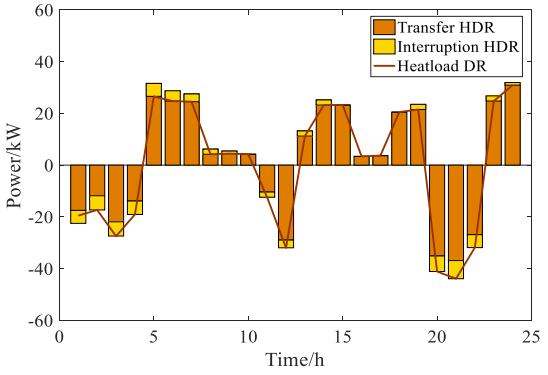


**FIGURE 6.** Day-ahead heating load DR.

heat load within the range of flexible temperature adjustment is realized, thus the energy supply pressure of the system is reduced.

### 2) ANALYSIS OF SYSTEM BALANCE

Fig. 7 (a) shows the change of electric load curve and the output balance of the system unit before and after the integrated DR. Considering that the peak-valley difference of the power load curve becomes smooth after the DR, combined with the analysis of the time-of-use electricity price information of each period, the power load increases in the periods of 22:00-24:00 and 1:00-9:00 at night. Due to the low electricity price in this period, after the wind consumption reaches the upper limit, the system buys electricity from the power grid for power storage. After cutting peak and filling valley, the power purchase from the system is reduced at 18:00-22:00 during the peak period of power load. The power load is mainly supplied by WP, and the shortage is made up by cogeneration units, battery discharge and power purchase from the power grid. The peak value decreases after the DR from 10:00 to 13:00, but the PV output power is larger in this period, mainly due to the balance of PV and WP supply, and PV can not be completely absorbed.

Fig. 7(b) shows the heat load change curve and the output of heat energy units before and after considering DR. Heating

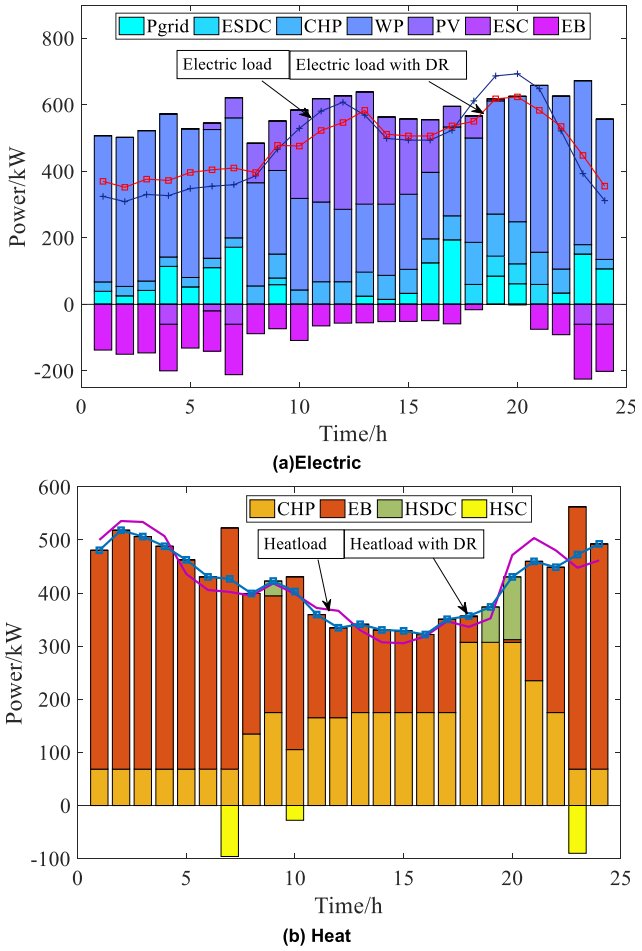


**FIGURE 7.** Electric and heat load balance before and after DR.

is mainly satisfied by CHP unit and EB. HS is an auxiliary equipment to participate in the heat network balance, and the output of each unit is related to the electricity price and the output of each unit in the power system. The output of heat load decreases during the period from 1:00 to 5:00, so the output of the CHP unit decreases and the consumption of WP at night is increased. The heat load output increases at 6:00-9:00 and 14:00-17:00, and it is considered to be supplemented by the addition of EB, which strengthens the PV absorption to a certain extent and improves the flexibility of system scheduling. The peak of electric power consumption from 19:00 to 22:00 reduces the demand for heat load and the output of EB. the heat load is mainly met by the heat release of CHP unit and heat storage tank to reduce the pressure of power system and improve the flexibility of system scheduling.

#### 3) ANALYSIS OF WIND AND PV ACCOMMODATION

Fig.8 shows the wind and PV output before and after considering DR. As can be seen from Fig.10, the wind and PV accommodation will be increased when DR is taken into account in the periods of 1:00-5:00 and 21:00-24:00 in the high power generation period of wind power and 10:00-15:00 in the period of sufficient PV energy. This is due to the fact

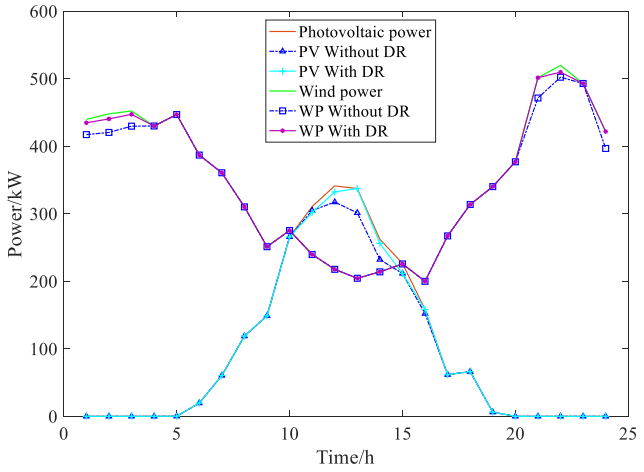


**FIGURE 8.** Wind and PV accommodation.

that the load after the DR is transferred in time, and the system unit increases the electricity consumption in the period of energy surplus by adjusting the output, which makes the wind energy more efficient.

## V. ANALYSIS OF INTRA-DAY OPTIMAL SCHEDULING

With the shortening of time scale, the forecasting accuracy of WP, PV and load is improved. Rolling optimal scheduling of ultra-short-term forecasting data is an effective means to reduce the impact of WP, PV and load forecasting errors on system scheduling. On the basis of the day-ahead scheduling plan, using the updated forecast information to further adjust the intra-day output of the distributed power supply(each unit), maintaining the power balance of the system while making the intra-day adjustment of each unit as small as possible is the main optimization goal of intra-day scheduling.

### A. EXAMPLE DATA

The system parameters in the intra-day optimal scheduling are the same as those in the previous chapter, and the scheduling time scale of the day-ahead scheduling is 1 hour, a total of 24 scheduling periods. The upper heat energy time scale of intra-day scheduling is 30 minutes and the scheduling results are transmitted to the lower layer. The lower power layer adjusts the system within 15 minutes as the scheduling cycle. The unit continues to roll and optimize and minimize the amount of adjustment. Considering the uncertain factors such as interference and meteorology, the wind output and load are predicted in ultra-short time. The forecast value of the day-ahead data has an error of about 15%, and the ultra-short time prediction error is small, which can improve the scheduling accuracy.

### B. ANALYSIS OF THE RESULTS OF INTRA-DAY OPTIMAL SCHEDULING

#### 1) ANALYSIS OF HEAT ENERGY ADJUSTMENT IN THE INTRA-DAY UPPER LAYER

Fig. 9 shows the heat DR of the intra-day upper layer. Intra-day load forecasting is more uncertain than day-ahead load

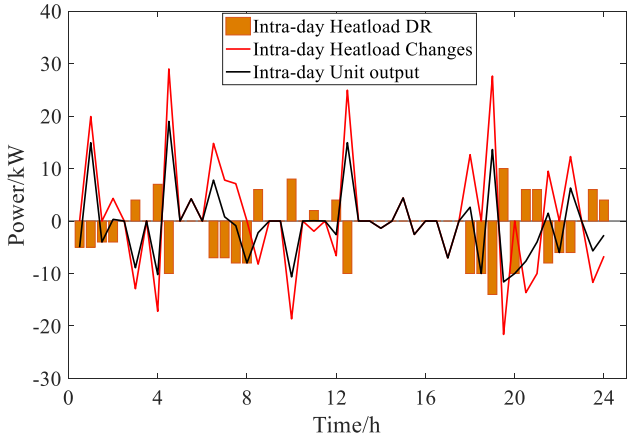


**FIGURE 9.** Intra-day upper layer heat load DR.

forecasting, and the total heat load of the system changes. When the load demand increases, the DR of the intra-day heat load decreases, otherwise it increases. The fluctuation of the DR load becomes smooth, which is beneficial to the stable scheduling of the system unit, and the residual fluctuation is balanced by the unit adjustment.

Fig. 10 shows the comparison of the adjustment of the upper scheduling units in the day-ahead and intra-day. The analysis shows that the load change is mainly balanced by the adjustment of CHP unit and EB. The overall electricity load demand increases from 1:00 to 4:00, so the output of the CHP unit increases. In other periods, the output of the EB unit and heat storage tank is slightly adjusted to balance the load fluctuation in a short time scale and maintain the stable operation of the system.

### 2) ANALYSIS OF POWER ADJUSTMENT IN THE INTRA-DAY LOWER LAYER

On the basis of intra-day upper-layer scheduling, the lower-layer real-time scheduling of electric energy is carried out. the WP, PV and load data are updated in 15 minutes. The class B IDR is adjusted to participate in the system's optimal scheduling in time. Fig. 12 shows the electric load fluctuation and the electric load DR under the short time scale, which is similar to the upper heat energy response, and the electric load DR smooths out the fluctuation of the electrical load.

After the DR, the lower power load fluctuation is mainly achieved through the CHP unit, batteries and interaction with the power grid to achieve balance. Because the output of the CHP unit is proportional to heat energy, the scheduling time of the CHP unit is limited. According to the output results, compared with the current battery operation state, due to the uncertainty of system wind, PV and load, the interaction between the battery and the power grid intra-day scheduling plan has a small adjustment to balance the system fluctuation and more accurately follow the system output.

To sum up, different types of DR have different response capabilities at different time scales, which can participate in system scheduling through coordination and cooperation to

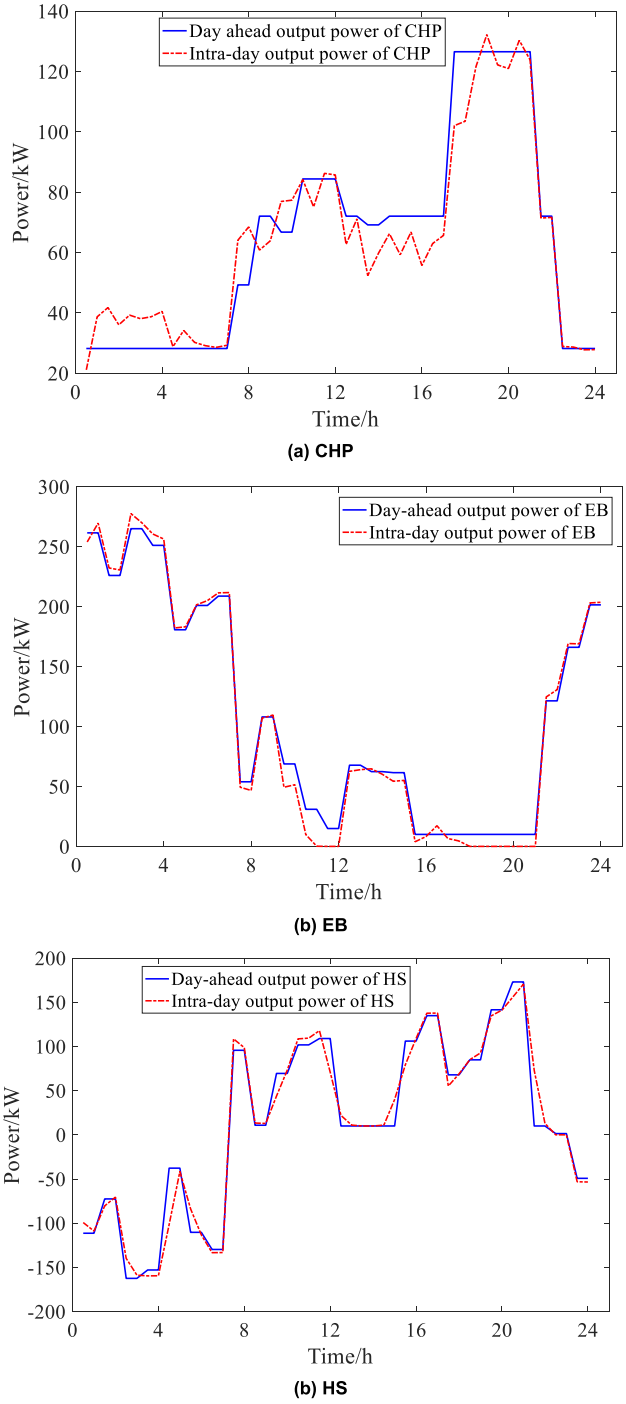


**FIGURE 10.** Adjustment results of upper unit intra-day.

reduce load fluctuations and reduce the difficulty of system unit adjustment. The adjustment of the power of the EB and the heat storage tank is relatively small in the process of intra-day rolling scheduling, which almost coincides with the day-ahead scheduling. While the storage battery and gas turbine have relatively large adjustments because of the fluctuation of load, wind and PV, and the power output has good following performance. The unit accurately follows the load

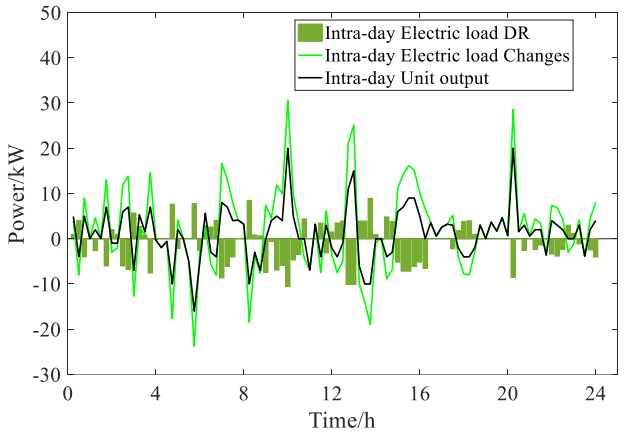


**FIGURE 11.** Intra-day lower layer electric load DR.

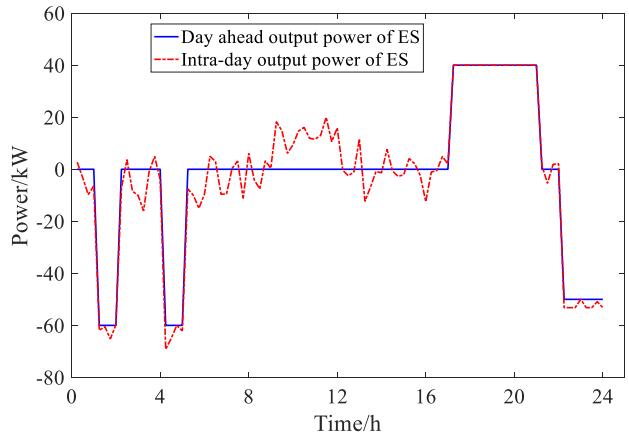


(a) ES

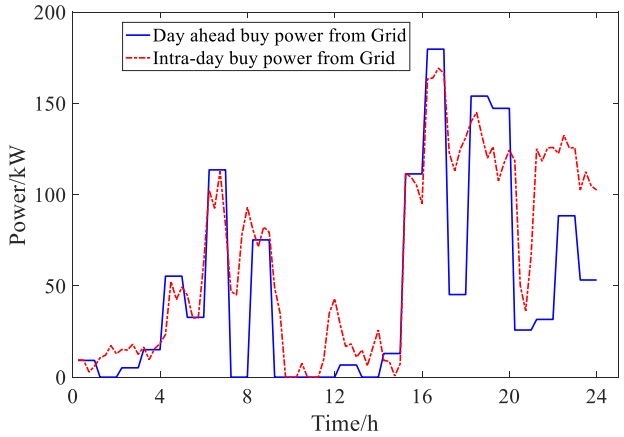


(b) Grid

**FIGURE 12.** Adjustment results of Intra-day lower layer.

fluctuation through coordinated scheduling, and the overall optimization effect is good. As a flexible and dispatchable power supply, the interaction between the battery and the power grid has the ability of rapid response. So it can quickly respond to the changes of WP, PV and load through the intra-day short-time scheduling scale, so as to stabilize the uncertain fluctuating power of the system and ensure the safe and stable operation of the system.

**TABLE 3.** System scheduling cost.

| Cost(yuan/day) | $C_{yun}$ | $C_{buy}$ | $C_Q$ | $C_{IDR}$ | $C$ |
|---|---|---|---|---|---|
| Scenario 1 | 621.7 | 1854.1 | 267.3 | 0 | 2740.1 |
| Scenario 2 | 741.5 | 1669.4 | 93.4 | 105.6 | 2609.9 |

### C. ADVANTAGES OF MULTI-TIME-SCALE OPTIMAL OPERATION STRATEGY

#### 1) SCENE SETTING

Scenario 1: Day-ahead phase DR considers PDR and class A IDR; Consider day-ahead heat DR.

Scenario 2: Day-ahead phase DR considers PDR and class A IDR; Consider day-ahead hot DR. Larger time scale (30mins) heat DR and shorter time scale class B IDR are considered in the intra-day phase.

#### 2) COST COMPARISON AND ANALYSIS

The total operating cost of the system before and after considering the multi-time-scale strategy is shown in Table 3. Due to the intra-day short-time scale scheduling, the unit adjustment frequency has increased, resulting in an increase in the unit scheduling cost. Considering the load demand adjustment, the system scheduling is flexible. The system energy purchase cost is reduced, and the scenery consumption is increased. Therefore, the penalty for abandoning wind and PV has been reduced. After considering the load demand incentive compensation, the total operating cost of the system is relatively reduced. It is verified that taking into account the multi-time-scale DR strategy can improve the operation economy of the system and increase the consumption of new energy.

## VI. CONCLUSION

In this paper, aiming at the optimal scheduling problem of IES, taking the lowest operating cost of the system as the objective function, the optimal scheduling model of IES with different types of DR under multi-time scale is established. In the day-ahead phase, the optimal economic day-ahead scheduling plan is made by considering PDR, class A IDR and heat DR. Class B IDR and short time scale heat DR are considered in the intra-day phase. Hierarchical optimization scheduling of heat energy and electric energy of the system by refining the time scale, and the intra-day adjustment plan is obtained. Through the simulation analysis and comparison of numerical examples, the following conclusions are obtained:

1) The proposed DR multi-time-scale response strategy takes into account the multi-time-scale characteristics of different energy types and the response ability of different DR resources, which improves the economy of electro-thermal IES operation. The intra-day optimal operation scheduling

model takes into account the response time characteristics of equipment, so that devices with different response capabilities can effectively participate in the intra-day scheduling plan, which is closer to the actual operation status of IES.

2) Considering the uncertainty of wind and PV, load forecast and DR with the change of scheduling time, the multi-time scale response strategy proposed in this paper. It effectively calms the fluctuation trend of the system, and gives full play to the role of DR in the regulation of power grid peak cutting and valley filling. Moreover, the strategy continuously modifies the unit output of the system to reduce the prediction error by establishing an optimal scheduling model of multi-layer cooperation in the day-ahead and intra-day stages, so as to ensure the safe and stable operation of the system. Furthermore, the economy and effectiveness of the scheduling strategy proposed in this paper are verified.

## CONFLICT OF INTEREST

All authors declare that there is no conflict of interest.

## AUTHOR CONTRIBUTIONS

JIAN TANG: Conceptualization, Research strategy, Writing-Original draft preparation. JIANFENG LIU: Writing- Original draft preparation. TIANXING SUN: Translation and Validation. HERAN KANG: Research strategy. XIAOQING HAO: Data curation.

## REFERENCES


[1] M. A. Gilani, A. Kazemi, and M. Ghasemi, "Distribution system resilience enhancement by microgrid formation considering distributed energy resources," *Energy*, vol. 191, Jan. 2020, Art. no. 116442.

[2] Z. Wang, J. Hu, and B. Liu, "Stochastic optimal dispatching strategy of electricity-hydrogen-gas-heat integrated energy system based on improved spectral clustering method," *Int. J. Electr. Power Energy Syst.*, vol. 126, Mar. 2021, Art. no. 106495.

[3] J. Li, M. Zhu, Y. Lu, Y. Huang, and D. Wu, "Review on optimal scheduling of integrated energy systems," *Power Syst. Technol.*, vol. 45, no. 6, pp. 2256–2269, 2021.

[4] P. Li, Z. Wang, J. Wang, W. Yang, T. Guo, and Y. Yin, "Two-stage optimal operation of integrated energy system considering multiple uncertainties and integrated demand response," *Energy*, vol. 225, Jun. 2021, Art. no. 120256.

[5] B. Qi, S. Zheng, Y. Sun, B. Li, S. Tian, and K. Shi, "A model of incentive-based integrated demand response considering dynamic characteristics and multi-energy coupling effect of demand side," *Proc. CSEE*, vol. 42, no. 5, pp. 1783–1799, Sep. 2022.

[6] A. T. Moghadam, F. Soheyli, S. Sanei, E. Akbari, H. Khorramdel, and M. Ghadamyari, "Bi-level optimization of the integrated energy systems in the deregulated energy markets considering the prediction of uncertain parameters and price-based demand response program," *Energy Sci. Eng.*, vol. 10, no. 8, pp. 2772–2793, Aug. 2022.

[7] Z. Xu, H. Sun, and Q. Guo, "Review and prospect of integrated demand response," *Proc. CSEE*, vol. 38, no. 24, pp. 7194–7205, 2018.

[8] B. Zeng, Y. Liu, F. Xu, Y. Liu, X. Sun, and X. Ye, "Optimal demand response resource exploitation for efficient accommodation of renewable energy sources in multi-energy systems considering correlated uncertainties," *J. Cleaner Prod.*, vol. 288, Mar. 2021, Art. no. 125666.

[9] W. Yuan, X. Wang, C. Su, C. Cheng, Z. Liu, and Z. Wu, "Stochastic optimization model for the short-term joint operation of photovoltaic power and hydropower plants based on chance-constrained programming," *Energy*, vol. 222, May 2021, Art. no. 119996.

[10] J. Priolkar and E. S. Sreeraj, "Analysis of price based demand response program using load clustering approach," *IETE J. Res.*, pp. 1–14, Jan. 2023.

[11] X. Zhu, Y. Sun, J. Yang, Z. Dou, G. Li, C. Xu, and Y. Wen, "Day-ahead energy pricing and management method for regional integrated energy systems considering multi-energy demand responses," *Energy*, vol. 251, Jul. 2022, Art. no. 123914.

[12] M. Majidi, B. Mohammadi-Ivatloo, and A. Anvari-Moghaddam, "Optimal robust operation of combined heat and power systems with demand response programs," *Appl. Thermal Eng.*, vol. 149, pp. 1359–1369, Feb. 2019.

[13] J. Wang, H. Zhong, Z. Ma, Q. Xia, and C. Kang, "Review and prospect of integrated demand response in the multi-energy system," *Appl. Energy*, vol. 202, pp. 772–782, Sep. 2017.

[14] N. I. Nwulu and X. Xia, "Optimal dispatch for a microgrid incorporating renewables and demand response," *Renew. Energy*, vol. 101, pp. 16–28, Feb. 2017.

[15] L. Wang, J. Lin, H. Dong, Y. Wang, and M. Zeng, "Demand response comprehensive incentive mechanism-based multi-time scale optimization scheduling for park integrated energy system," *Energy*, vol. 270, May 2023, Art. no. 126893.

[16] L. W. Ju, C. Qin, and H. L. Wu, "Wind power accommodation stochastic optimization model with multi-type demand response," *Power System Technol.*, vol. 39, no. 7, pp. 1839–1846, 2015.

[17] Z.-S. Zhang, Y.-Z. Sun, D. W. Gao, J. Lin, and L. Cheng, "A versatile probability distribution model for wind power forecast errors and its application in economic dispatch," *IEEE Trans. Power Syst.*, vol. 28, no. 3, pp. 3114–3125, Aug. 2013.

[18] Z. Pan, Q. Guo, and H. Sun, "Interactions of district electricity and heating systems considering time-scale characteristics based on quasi-steady multi-energy flow," *Appl. Energy*, vol. 167, pp. 230–243, Apr. 2016.

[19] H. Liu, Y. Zhao, C. Gu, S. Ge, and Z. Yang, "Adjustable capability of the distributed energy system: Definition, framework, and evaluation model," *Energy*, vol. 222, May 2021, Art. no. 119674.

[20] X. Li, W. Wang, and H. Wang, "Hybrid time-scale energy optimal scheduling strategy for integrated energy system with bilateral interaction with supply and demand," *Appl. Energy*, vol. 285, Mar. 2021, Art. no. 116458.

[21] Y. Wu, X. Zhang, and H. Sun, "A multi-time-scale autonomous energy trading framework within distribution networks based on blockchain," *Appl. Energy*, vol. 287, Apr. 2021, Art. no. 116560.

[22] P. Li, Z. Wang, J. Wang, T. Guo, and Y. Yin, "A multi-time-space scale optimal operation strategy for a distributed integrated energy system," *Appl. Energy*, vol. 289, May 2021, Art. no. 116698.

[23] D. F. Yang, Y. Xu, and C. Jiang, "Multple time-scale coordinated scheduling of combined electro-thermal system considering multi-type demand response," *Acta Energiae Solaris Sinica*, vol. 42, no. 10, pp. 282–289, 2021.

[24] Z. C. Jiang, T. Y. Liu, and X. C. Jiang, "Multi-time scale home energy management optimization stratery in smart grid," *Acta Energiae Solaris Sinica*, vol. 42, no. 1, pp. 460–469, 2021.

[25] H. Yang et al., "Multi-time scale optimal scheduling of regional integrated energy systems considering integrated demand response," *IEEE Access*, vol. 99, pp. 1–10, 2020.

[26] J. Wu, X. Li, Y. Lin, Y. Yan, and J. Tu, "A PMV-based HVAC control strategy for office rooms subjected to solar radiation," *Building Environ.*, vol. 177, Jun. 2020, Art. no. 106863.

[27] J. Cheng, Z. Tan, and L. Yue, "CCHP-SESS bi-layer optimal configuration considering load comprehensive demand response," *Power Syst. Technol.*, vol. 47, no. 3, pp. 918–931, 2023.


**JIAN TANG** was born in Zhenping, Henan, China, in December 1967. He received the bachelor's degree in relay protection and automatic telecontrol technology from North China Electric Power University, in 1990. He was recognized as a Senior Engineer, in 2001. He is currently the Director of the Economic and Technological Research Institute, State Grid Inner Mongolia Eastern Electric Power Company Ltd. He has published a total of five articles and authorized three invention patents. His research interest includes power system and its automation.

**JIANFENG LIU** was born in Hulunbuir, Inner Mongolia, in March 1993. He received the bachelor's degree from the Inner Mongolia University of Science and Technology, in 2015, and the master's degree from the Harbin Institute of Technology, in 2018. After graduation, he has been engaged in the research and development of scientific and technological projects with the Economic and Technological Research Institute, State Grid Inner Mongolia Eastern Electric Power Company Ltd. In 2022, he became an on-the-job doctoral candidate of Shenyang University of technology. He has published four core papers and authorized four invention patents. His research direction is multi physical field coupling modeling and analysis.

**TIANXING SUN** was born in Da'an, Jilin, in April 1993. He received the bachelor's degree from North China Electric Power University, in 2015. Since 2015, he has been with the Economic and Technical Research Institute, State Grid Inner Mongolia Eastern Electric Power Company Ltd., responsible for pre-project work and administrative management of power grid projects. He has prepared more than 20 project approval reports and obtained one authorized patent. His research interest includes power grid planning.

**HERAN KANG** was born in Inner Mongolia, China, in February, 1989. He received the degree in electrical engineering and automation from Beijing Jiaotong University, in 2011, and the master's degree in electrical engineering from the Inner Mongolia University of Technology, in 2016. Since 2016, he has been engaged in power grid planning with the Economic and Technological Research Institute, State Grid Inner Mongolia Eastern Electric Power Company Ltd. He prepared more than 20 planning reports. He has published three Chinese core articles and authorized seven patents. His research interest includes power grid planning.

**XIAOQING HAO** was born in Hohhot, Inner Mongolia, in September, 1986. He received the bachelor's degree in electrical engineering and automation from Inner Mongolia University of Science and Technology. In recent years, he has been engaged in the research work in the field of lightning protection detection of new energy power station and comprehensive utilization of new energy. In the field of electro-thermal coupled multi-energy flow system, there are many demonstration projects. He is engaged in research work in the field of new energy power generation in Inner Mongolia Hengsheng New Energy Technology Company Ltd. He published two academic papers and two patents were authorized.